Evolution of 2,5-Bis(4-biphenylyl)bithiophene Thin Films and Its Effect on the Weak Epitaxy Growth of ZnPc

ARTICLE *in* THE JOURNAL OF PHYSICAL CHEMISTRY B · MARCH 2010

Impact Factor: 3.3 · DOI: 10.1021/jp100095r · Source: PubMed

6 AUTHORS, INCLUDING:

Lizhen Huang
Soochow University (PRC)
27 PUBLICATIONS **339** CITATIONS
SEE PROFILE

Jidong Zhang
Chinese Academy of Sciences
101 PUBLICATIONS **1,106** CITATIONS
SEE PROFILE

Evolution of 2,5-Bis(4-biphenylyl)bithiophene Thin Films and Its Effect on the Weak Epitaxy Growth of ZnPc

Lizhen Huang, Chengfang Liu, Bo Yu, Jidong Zhang, Yanhong Geng, and Donghang Yan*

State Key Laboratory of Polymer Physics and Chemistry, Changchun Institute of Applied Chemistry, Chinese Academy of Sciences, and Graduate School of Chinese Academy of Sciences, Changchun 130022, People's Republic of China

Received: January 5, 2010; Revised Manuscript Received: March 2, 2010

Evolution of BP2T films grown at the early stage was investigated using atomic force microscopy (AFM) and X-ray diffraction (XRD). The AFM results demonstrate that the BP2T grown on the SiO_2 substrate transformed from a layer by layer growth to island growth when the coverage is higher than 3 ML. The out-of-plane and in-plane X-ray diffraction measurements reveal a phase transition from the thin film phase to the bulk phase suddenly occurs as the growth mode changes. A careful analysis of the structure evolution implies that not only the strain but also the soft matter property of the organic thin films are responsible for the thickness dependent evolution. Moreover, the thickness dependent structure and phase of BP2T films result in different morphologies of ZnPc grown on different layers of BP2T. The ZnPc crystals gradually changed from stripe-like to nanofiber-like, concomitantly with the epitaxy relationships from incommensurate epitaxy to commensurate epitaxy. Conversely, the diversity of ZnPc films also reflects different properties of the BP2T films with different numbers of layer, which cannot be obtained from the AFM or XRD. This study supplies a deeper insight into the thickness evolution of organic thin films and to the weak epitaxy growth.

1. Introduction

Organic semiconductor films have attracted tremendous attention in recent decades owing to the potential application in organic electronics, such as organic thin film transistors, organic solar cells, and sensors.[1−3] The device performances show closely relations to the quality of organic thin film. Attempts such as optimizing the film growth condition, introducing epitaxy technique or using an oriented substrate (such as PTFE) have been reported to improve the films quality and further to improve the device performance.[4−9] Recently, weak epitaxy growth (WEG) has been developed by introducing an ordered *p*-6P layer between the substrate and organic films and elevate substrate temperature.[10] Highly oriented and ordered organic semiconductor films can be obtained by the WEG method.[11−14] The mobility of transistors based on the WEG films can be achieved at the same level of their corresponding single crystals.[15]

Although the *p*-6P as the inducing layer has been successfully applied to fabricate high performance transistors, its large band gap and low mobility prevent it from application in the organic photovoltaic cells (OPV) in which the charge carrier transport is in the direction normal to the film plane. Recently, a new inducing molecule, 2,5-bis(4-biphenylyl)bithiophene (BP2T), was introduced to weak epitaxy growth of ZnPc, by which a highly efficient organic solar cell was obtained.[16] BP2T is a thiophene/phenylene co-oligomer with a zigzag shape that possesses a suitable energy level and high mobility (Figure 1).[17−19] An important reason for the highly efficient OPV is that the BP2T films could present a very smooth surface even at a thickness up to 8 nm (near three layers), which avoids the appearance of pinholes but induces the formation of high quality ZnPc films at the same time. This is different from the *p*-6P, which only presents smooth films on the monolayer grown on an optimized substrate temperature.[20] However, details about the BP2T film grown on the inert substrate and further the mechanism of organic thin films evolution as thickness are still unclear, such as the growth mode transition or the phase transition.[21−23] On the other hand, the film evolution with thickness might greatly influence the weak epitaxy growth behavior of organic semiconductors and the device performance. In this report, using the atomic force micrograph (AFM), X-ray diffraction (XRD) and transmission electron microscope (TEM), we systemically study the morphology and structure evolution of the BP2T thin film growth in the early stage, and its effect on the weak epitaxy growth behavior of ZnPc. The results show that the BP2T films undergo a growth mode change as the thickness increases to 3 ML, concomitant with a phase transition. This evolution was found not only to be driven by the strain but also to be closely related to the soft matter property of organic materials. Moreover, the thickness dependent structure and phase of BP2T films result in diverse morphologies of ZnPc epitaxilly grown on different layers of BP2T.

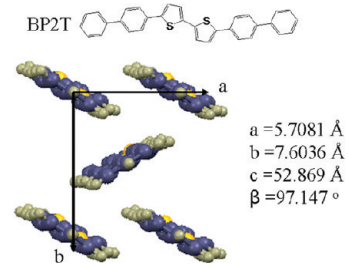

Figure 1. Molecular structure of BP2T and its crystal packing of (001) plane.

* Corresponding author. E-mail: yandh@ciac.jl.cn. Fax: +86-431-85262266. Tel: +86-431-85262165.

10.1021/jp100095r
Published on Web 03/19/2010

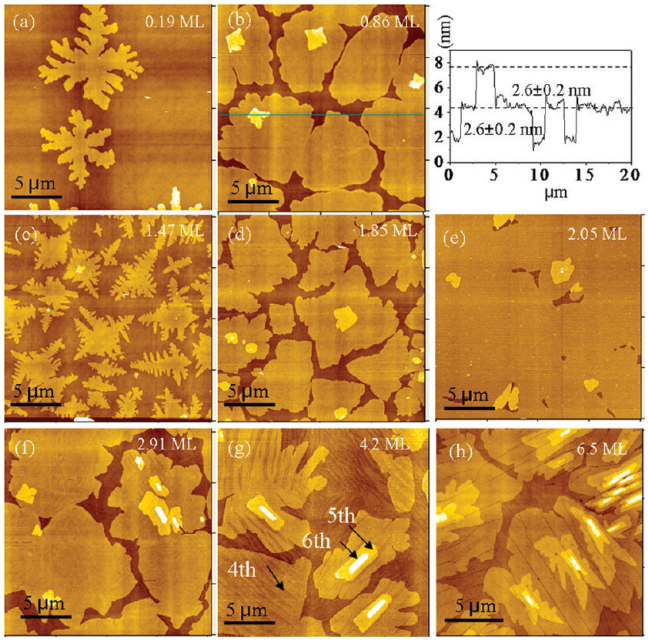

Figure 2. AFM topography images of BP2T with different coverage on the SiO_2/Si substrate: (a) 0.19 ML; (b) 0.86 ML; (c) 1.47 ML; (d) 1.85 ML; (e) 2.05 ML; (f) 2.91 ML; (g) 4.2 ML; (h) 6.5 ML. Height profile of the solid line in (b).

2. Experimental Section

2.1. Fabrication of Organic Thin Films. Commercial zinc phthalocyanine was purchased from Aldrich Co., and the BP2T was synthesized according to ref 24. Prior to experiments all the materials were purified twice by thermal gradient sublimation. A heavily doped n-type silicon wafer with a 300 nm thermal oxidation SiO_2 layer was used as the substrates. First, BP2T films with varied thicknesses were deposited on the SiO_2 substrate. Then, ZnPc with different thicknesses were deposited on the BP2T thin films. The deposition was performed under pressure of 10^{-4} to 10^{-5} Pa at a rate of about 1 nm/min with a substrate temperature at 155 °C.

2.2. AFM Measurements. Film morphologies were imaged by a SPI 3800/SPA 300HV (Seiko Instruments Inc., Japan) with tapping mode. A 150 μm scanner and a commercially available SiN_4-cantilever with a spring constant of 2 N/m were used.

2.3. XRD Measurements. The out-of-plane XRD patterns were taken from a D8 discovery thin-film diffractometer with Cu Kα radiation (λ = 1.540 56 Å). The selected voltage and current were 40 kV and 40 mA, respectively. The in-plane pattern was performed by the GIXD measurements using the synchrotron radiation (λ = 1.24 Å) at BL14B1 at Shanghai Synchrotron Radiation Facility (SSRF).

2.4. TEM Measurements. Organic films were first deposited on the SiO_2 substrate, subsequently a carbon thin film used as a support layer was deposited on the films. The films were separated from the SiO_2 surface by floating from 10% HF solution and then were transferred to a copper grid for measurements. Au directly deposited on the samples for demarcating if necessary. The selected area electron diffraction was performed by a JEOL JEM-1011 transmission electron microscope operated at 100 kV. Dark field was used for experiments to provide weaker-intensity beam and high contrast.

3. Results and Discussion

3.1. Growth Behavior and Structure Evolution of BP2T Thin Films. Figure 2a−h shows the morphology evolution of BP2T films with different coverage under a substrate temperature of 155 °C (this temperature is optimized through experiment like *p*-6P, and lower than the optimized temperature (180 °C) of *p*-6P, which is owing to their different thermal properties).[25] In the early stages, fractal islands formed on the SiO_2 substrate (Figure 2a) and then changed to dendritic and compact islands as the coverage increases (Figure 2b), similar to the growth behavior of the *p*-6P monolayer. Simultaneously, when the coverage increased to 0.86 ML, coalescence between compact islands took place and the nucleus of a second layer began to form, which implies that the first layer is two-dimensional growth (layer-by-layer growth). According to the height profiles of the film, the layers' height is around 2.6 ± 0.2 nm, comparable to the long axis of the BP2T molecule, which indicates the BP2T molecule is upright on the SiO_2 substrate with the long molecular axis normal to the substrate surface. The growth of the BP2T first layer is the same as for the *p*-6P monolayer, but from the second layer, a different morphology is observed. As parts c and d of Figure 2 show, different from the island growth of the *p*-6P second layer, the second layer of BP2T also presents behavior similar to that of the first layer and remains the layer by layer growth mode. When the coverage increases to 2.05 ML (Figure 2e), large size domains of the second layer are obtained. As Figure 2e shows, in the image area (20 μm × 20 μm) all the domains coalesce and form a flat surface with a root-mean-square roughness (rms) of 1.0 nm. Further increasing the coverage, we find the layer-by-layer growth manner can be retained until the third layer (Figure 2f) grows. As the fourth layer begins to grow, the fifth or sixth layer also appears, reflecting the growth fashion change to the island growth (Figure 2g,h). Furthermore, the initial islands of the fourth or higher layer present a regular stripe shape similar to that of the bulk crystal.

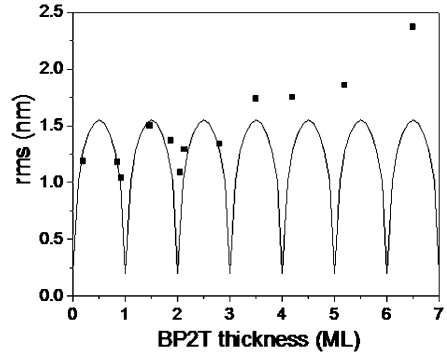

Figure 3. Rms as a function of the coverage.

The evolution of the root-mean-square roughness (calculated from the AFM images) as a function of the coverage (Figure 3) further reflects the growth model transition. The solid line is the theoretical evolution of the rms for an ideal layer by layer growth on the substrate (the rms of the SiO_2 substrate here is 0.2−0.3 nm). As Figure 3 shows, the rms agrees with the ideal layer by layer growth when the coverage is below 3 ML but deviates when the coverage is higher than 3 ML.

Previous work of *p*-6P pointed out that the *p*-6P monolayer grown with the layer-by-layer mode is different from its bilayer film with island growth. The bilayer film is approximately the bulk phase, while the monolayer might be a high order liquid-like phase named the thin film phase. Here, the first three layers of BP2T show growth behavior similar to that of the *p*-6P monolayer. Hence the film structure in the first three layers might be different from the subsequent

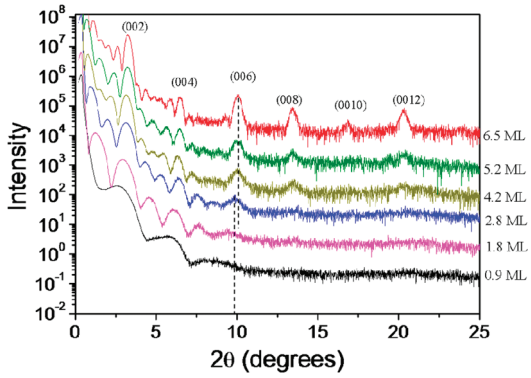

Figure 4. Out-of-plane X-ray diffraction patterns of BP2T with different coverage.

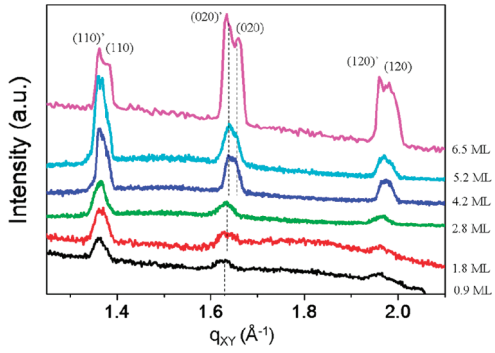

Figure 5. In-plane GIXD patterns of BP2T films with different coverages.

films grown under island growth. Other groups have reported the film structure of organic molecules would gradually change as the thickness increased and then remain constant as the island growth appearred.[22,23] To thoroughly understand the film evolution as the thickness, X-ray diffraction is performed to investigate the out-of-plane and in-plane structure evolution as thickness.

Figure 4 shows the out-of-plane diffraction patterns. Appearance of (00*l*) plane diffraction confirms the molecule is standing up on the substrate (for the film lower than 1 ML, only thickness interference peaks present). An obvious shift of the (006) diffraction peak was observed as the coverage changed from 2.8 to 4.2 ML. The corresponding lattice space was changed from 8.96 to 8.77 Å. The latter is nearly equal to the value of the bulk phase (8.74 Å). It reveals that the structure of the first three layers is indeed different from the subsequent layer or the bulk phase. Similarly to most organic thin films such as pentacene, we defined the structure below 3 ML as the "thin film phase". Besides, the structure evolution is a sudden change not a gradual change, which has been reported in some organic molecules. The change of structure is coincident with the transition from layer-by-layer growth to island growth.

The in-plane structure evolution is tested by the GIXD measurements using synchrotron radiation. As Figure 5 shows, the diffraction patterns of all the films show three diffraction peaks that correspond to the (110), (020), and (120) (for the thin film phase is (110)′, (020)′, (120)′), respectively. Similarly, significant change is also observed as the coverage changes from 2.8 to 4.2 ML. Figure 6 shows the evolution of lattice space as the coverage, and the two dashed lines corresponding to the $d_{(010)}$ and $d_{(100)}$ of the bulk phase. The films below 3 ML show only one structure with

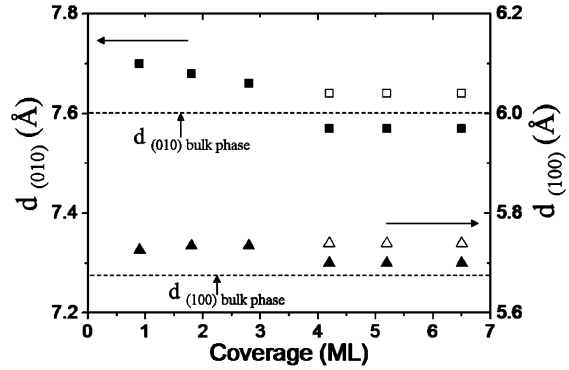

Figure 6. Evolution of lattice parameters as the function of coverage.

the lattice space larger than the bulk phase. And a slight shift of the $d_{(010)}$ was observed. At coverages higher than 4.2 ML, two structures coexist in the films. One is the thin film phase of the initial three layers (the hollow spots). The newly appearing structure corresponds to the fourth or higher layer, which shows a lattice parameter close to the value of the bulk phase. A significant change of $d_{(010)}$ and $d_{(100)}$ suddenly occurs as the fourth layer grows, which agrees well with the result of the out-of-plane diffraction. In addition, the thin film phase exhibits expanded lattice parameters compared to the bulk phase, revealing a more loose packing structure.

The X-ray diffraction results indicate that the first three layers exhibit a different phase from the subsequent layer. The structure evolution process reveals that phase transition from the thin film phase to the bulk phase is a sudden change that is strictly concomitant with the growth transition from layer-by-layer to island growth. The mechanism of the formation of thin film phase and the transition is unclear yet. Strain, which is the driving force in the inorganic system, has been reported as one factor to drive such a transition. But owing to the amorphous property of the SiO_2 substrate, no lattice mismatch exists here. The stain might not be enough to explain the structure evolution and the phase transition.[23] Furthermore, the organic molecule is greatly different from the inorganic materials. Previous work about the *p*-6P pointed out that the monolayer film might be an ordered phase of liquid-like crystal that favored the formation of large-size domains and layer-by-layer growth.[20] The liquid-like property might also be responsible for the evolution of BP2T thin films. Owing to the weak intermolecular interaction, large anisotropy, and the size effect, organic thin films, especially the first few layers, may present some soft matter property, such as the liquid-like property. Jiang and Ellison reported that the melting temperature or glass transition temperature of organic materials will greatly decrease as the film thickness decreased to a critical thickness.[26−28] Thin films below the critical thickness grown at high substrate temperature might present a liquid-like behavior and form a thin film phase. For the BP2T here, the critical thickness is up to three layers (the critical thickness is sensitive to the substrate temperature) better than the pentacene or *p*-6P. For the films below 3 ML, the large grain growth is favorable and grain coalescence is easy, which benefits from the liquid-like property, thus layer by layer growth is dominant. Once the film thickness is higher than the critical thickness, the liquidity rapidly decreases, and the films present crystal behavior. Hence, island growth appears, which results in forming a bulk phase. In addition, owing to the thickness

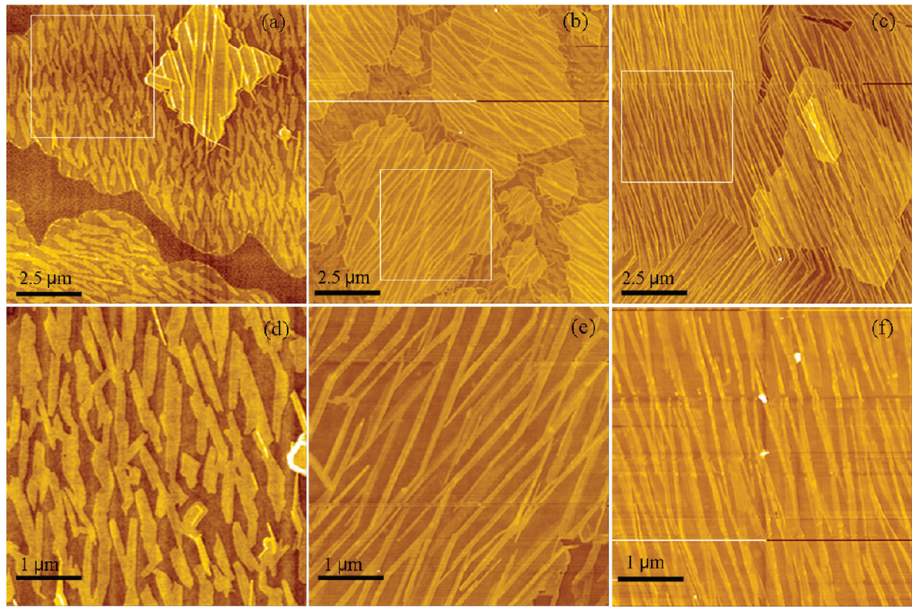

Figure 7. AFM topography of 1.0 nm ZnPc grown on BP2T first, second, and third layer: (a) ZnPc/BP2T monolayer; (b) ZnPc/BP2T bilayer; (c) ZnPc/BP2T trilayer; (d)−(f) the corresponding zoom images of (a)−(c).

dependent thermal property, the films might display different properties as the molecular layers increase.

3.2. Heteroepitaxy Growth Behavior of ZnPc on BP2T Films with Different Layers. The large grain size and good layer-by-layer growth behavior of BP2T in the first three layers made it a good inducing layer for the WEG method. Although the first three layers are layer-by-layer growth, a difference might exist between them owing to the thickness dependent properties such as the surface energy and the ordering. From the XRD results, only a slight shift of lattice space is observed, which is inadequate to reveal the difference. On the other hand, in the epitaxy growth technique, the orientations and morphologies of the epitaxial layer are critically controlled by the underlying inducing layer. The thickness evolution of the BP2T film will greatly influence the growth behavior of ZnPc. From a different perspective, morphology of ZnPc could be a demarcation for the different layer of BP2T grown at the early stage.

Figure 7 shows the AFM morphologies of 1.0 nm ZnPc deposited on a different layer of BP2T (monolayer, bilayer, and trilayer). Morphologies of the ZnPc crystals exhibit extraordinary differences as the number of layers of BP2T increases. On the BP2T monolayer, stripe-like crystals are present. The stripe crystals show a twist shape and wet the substrate, which is similar to the liquid behavior (Figure 7a,d). As the layer of BP2T is thicker than the double layer, fiber-like crystals with regular shapes are clearly observed (Figure 7b,c,e,f). The crystals are strongly anisotropic with a length-to-width ratio of about 20−30. Two preferential in-plane orientations are observed, crystals of the two orientations cement when they impinge, resulting in a sharp transition. However, a difference also exists between the fiber-like crystals on the second layer and third layer. The angle of the two in-plane orientations greatly diminishes, and the length of needle crystals increases as the layer of BP2T changes from the second layer to third layer. When the the number of layers of BP2T is further increased, the in-plane orientations show nearly only one needle (Figure 7c). Besides, all the morphologies are different from the morphology directly grown on SiO_2, which is random oriented crystals with small grain size.[10]

Further analyzing the crystals of ZnPc, we find that the nucleation density of ZnPc on different layers of BP2T is $N_{\text{trilayer}} \sim N_{\text{bilayer}} < N_{\text{monolayer}}$, and the length of crystals is $L_{\text{trilayer}} > L_{\text{bilayer}} > L_{\text{monolayer}}$, which indicates that the diffusion ability of ZnPc on the BP2T surface is $D_{\text{trilayer}} > D_{\text{bilayer}} > D_{\text{monolayer}}$. The height distributions of the crystals obtained by statistical data from the AFM images are also taken into account. Two peaks were observed as fitting data by the gauss function, the first peak corresponding to the mean height of the substrate layer; hence the discrepancy of two peak value in the height distribution curve gives the mean height of ZnPc crystals. The height distribution suggests that ZnPc crystals on the first layer present an average height of 1.4 nm, near the length of the ZnPc molecule, indicating that ZnPc shows layer-by-layer growth in the early few layers (Figure 8). However, on the BP2T second and third layer, the mean height of the ZnPc crystal is up to 2.8 nm, indicating that the ZnPc shows the three-dimensional growth mode. All the results imply that the BP2T surfaces of first, second, and third layer are different, although they are all thin film phases. As section 3.1 shows, the lattice space of (010) plane slightly decreases from the first layer to the third layer, indicating the more dense structure as the layer number increases. Furthermore, the second layer and third layer, which homoepitaxially grow on the first layer, present higher order than the first layer, which grows on the SiO_2 substrate. Thus on the BP2T second and third layer, the ZnPc molecule could diffuse to its favorite site ((010) plane of ZnPc) before being absorbed by the substrate layer, forming fiber-like crystals. Such considerable diversification indirectly revealed that the film structure of BP2T films gradually changed toward higher order as the layer number increased.

Select area electron diffraction (SAED) experiments were performed to investigate the epitaxy relationship between ZnPc and BP2T, and to further inquire into the influence of the inducing layer on the WEG growth behavior. Figure 9 shows SAED patterns of 5 nm ZnPc grown on different layers of BP2T. The indexed electron diffraction patterns consist of one [001] zone of BP2T and [100] zones of ZnPc. For the BP2T films, strong diffraction of (020) and (110) indicates that BP2T films

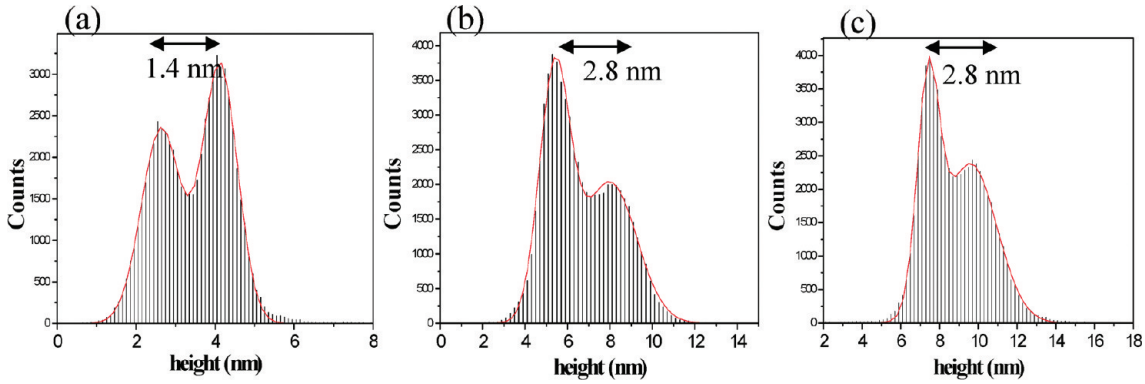

Figure 8. Height distribution of (a) Figure 7d (ZnPc/BP2T monolayer), (b) Figure 7e (ZnPc/BP2T bilayer), and (c) Figure 7f (ZnPc/BP2T trilayer).

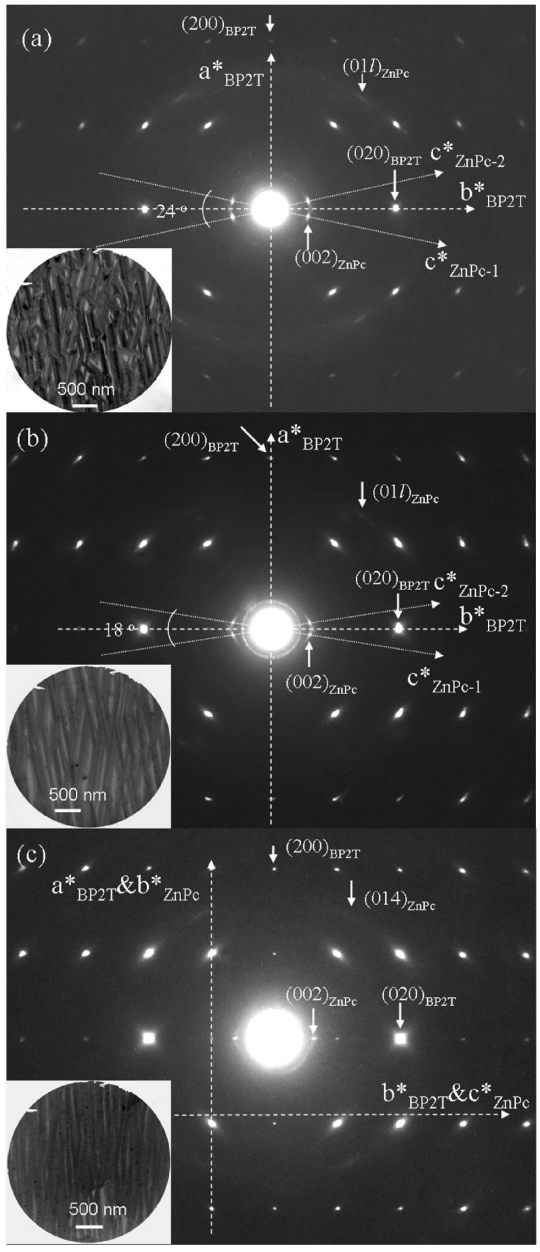

Figure 9. Select area electron diffraction pattern of (a) ZnPc(5 nm)/BP2T monolayer, (b) ZnPc(5 nm)/BP2T bilayer, and (c) ZnPc(5 nm)/BP2T trilayer.

are highly ordered with the (001) plane in contact with the SiO_2 substrate. Similar to the ZnPc grown on *p*-6P, diffraction spots of (002) and (01*l*) planes appear, which indicates the fiber-like crystals contact with the BP2T substrate by the (100) plane. Moreover, in each domain of BP2T monolayer and second layer, ZnPc crystals present two sets of in-plane orientations such that the angles between the *c** axes of ZnPc and the *b** axes of BP2T are ±12° and ±9°, respectively. According to the epitaxy grammar and our previous work, there is only an orientational relationship but no lattice matching between the ZnPc and BP2T; hence such epitaxy is incommensurate. While on the BP2T third layer, ZnPc crystals mainly present one set of in-plane orientation such that the *c** axis of ZnPc is parallel to the *b** axis of BP2T. Epitaxy relationship of this orientation is as follows: $(100)_{ZnPc} \parallel (001)_{BP2T}$, $[001]_{ZnPc} \parallel [010]_{BP2T}$, $[010]_{ZnPc} \parallel [100]_{BP2T}$. In addition, the two contact surfaces ($(100)_{ZnPc}$ and $(001)_{BP2T}$) possess the same symmetry, which results in a perfect lattice matching between them. In other words, this orientation corresponds to commensurate epitaxy.

According to the SAED results, the arrangement of ZnPc molecules on different layers of BP2T is analyzed. As our previous work mentions, the phthalocyanine molecules tend to nucleate along the geometrical channels formed by the prominent H atoms of the inducing layer. For the BP2T films, the geometrical channels formed by the prominent H atoms are [110] and [$\bar{1}$10], with a channel distance of 4.54 Å and an angle of about 108° in the bulk phase. For the ZnPc grown on the BP2T monolayer, the deviation of 20° is formed between the angle of the herringbone packing in ZnPc (128°) and the angle between the channels. As we know, the *c** axis of ZnPc forms an angle of 12° with respect to the *b** axis of BP2T, which can be achieved by a column of ZnPc molecules arranging on the [110] channel with its molecular plane deviated 2° with the [110] direction; the opposite molecules arrange on the [$\bar{1}$10] channel with a deviation of 22° (Figure 10a). On the BP2T bilayer, the angle between the *c** axis of ZnPc and *b** axis of BP2T decreases to 9°, which means a column of ZnPc arranges on the [110] channel with its molecular plane deviated 1° with the [110] direction; the opposite molecules arrange on the [$\bar{1}$10] channel with a deviation of 19° (Figure 10b). On the third layer of BP2T, the ZnPc molecules plane deviated from the [110] or [$\bar{1}$10] direction with an angle of 10°, which is larger than that on the first and second layer of BP2T (Figure 10c). Figure 10d shows the angle between the molecular plane respect to the [110] channel as the inducing layer increases. On the BP2T first and second layer, ZnPc molecules mostly arrange along the geometry channel of the substrate surface, indicating that the channel effect dominated the nucleation and growth, leading to incommensurate epitaxy. For the orientations corresponding to the commensurate epitaxy observed on the BP2T third layer, the

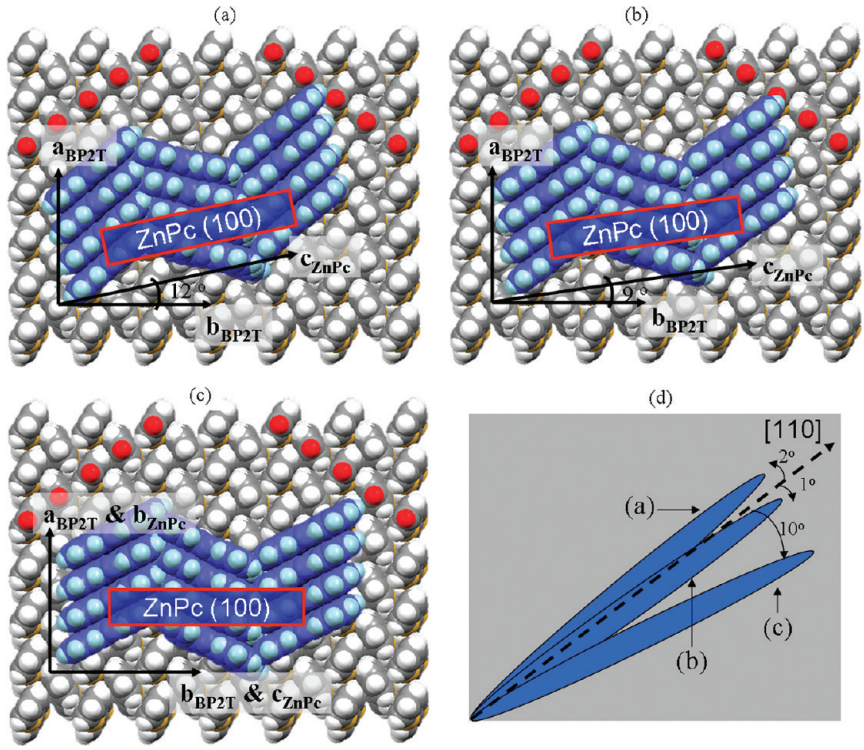

Figure 10. Schematic diagram of the ZnPc epitaxial grown on BP2T with various thickness: (a) ZnPc/BP2T (monolayer); (b) ZnPc/BP2T (bilayer); (c) ZnPc/BP2T (trilayer) (top view). (d) Derivation of molecule plane of ZnPc relative to the [110] channel of BP2T in the (a)−(c) situations, the dashed line corresponds to the [110] direction of BP2T.

effect of lattice matching between the substrate and the overlayer is not geometry channel determined by the growth of ZnPc. In addition, commensurate epitaxy is energetically most favorable, so as once such epitaxy appears, its growth is the most favored. Thus, on the third layer of BP2T, the two orientations will change to only one orientation corresponding to the commensurate epitaxy. The discrepancy of the epitaxy relationship reflects that the diffusion ability of ZnPc on the BP2T first and second layers is worse than that on the BP2T third layer. In other words, the BP2T films are becoming ordered as the layer number increased, which agrees with the above results.

4. Conclusions

In summary, evolution of a BP2T film grown in the early stage is investigated, and its effect on the epitaxy behavior of ZnPc is also studied. BP2T films grown at high substrate temperature present layer by layer growth up to 3 ML, and then change to island growth. The structure evolution as the thickness indicates that concomitantly with the growth mode change, phase transition from thin film phase to bulk phase critically occurs. A careful analysis of the film evolution implies that not only the thickness dependence strain but also the soft matter property of the organic materials are responsible for the thickness dependent phase and structure transition. Furthermore, the weak epitaxy growth behavior of ZnPc on the BP2T is sensitive to the number of layers of BP2T owing to the thickness dependent property. As the layer number of BP2T increases, the crystals of ZnPc changed from stripe-like to fiber-like with regular shape and their corresponding epitaxy relationship changes from incommensurate epitaxy to commensurate epitaxy. Conversely, different morphologies of ZnPc also reflect the BP2T films becoming ordered as the layer number increases. This study supplies more information to understand the thickness dependent growth behavior and weak epitaxy behavior of organic molecules, which will benefit optimization of organic devices.

Acknowledgment. This work was financially supported by the National Natural Science Foundation of China (50773079 and 50803063) and The National Basic Research Program (2009CB939702). The GIXD measurement was supported by the Shanghai Synchrotron Radiation Facility (SSRF).

Note Added after ASAP Publication. This paper was published ASAP on March 19, 2010. Text changes were made to the abstract, conclusions, and caption of Figure 8. The updated paper was reposted on March 24, 2010.

References and Notes

(1) Dimitrakopoulos, C. D.; Malenfant, P. R. L. *Adv. Mater.* **2002**, *14*, 99.
(2) Liu, S.; Wang, W. M.; Briseno, A. L.; Mannsfeld, S. C. B.; Bao, Z. *Adv. Mater.* **2009**, *21*, 1217.
(3) Forrest, S. R. *Nature* **2004**, *428*, 911.
(4) Bao, Z.; Lovinger, A. J.; Dodabalapur, A. *Appl. Phys. Lett.* **1996**, *69*, 3066.
(5) Forrest, S. R. *Chem. Rev.* **1997**, *97*, 1793.
(6) Andreev, A.; Matt, G.; Brabec, C. J.; Sitter, H.; Badt, D.; Seyringer, H.; Sariciftci, N. S. *Adv. Mater.* **2000**, *12*, 629.
(7) Koller, G.; Berkebile, S.; Krenn, J. R.; Netzer, F. P.; Oehzelt, M.; Haber, T.; Resel, R.; Ramsey, M. G. *Nano Lett.* **2006**, *6*, 1207.
(8) Campione, M.; Caprioli, S.; Moret, M.; Sassella, A. *J. Phys. Chem. C* **2007**, *111*, 12741.
(9) Wittmann, J. C.; Smith, P. *Nature* **1991**, *352*, 414.
(10) Wang, H. B.; Zhu, F.; Yang, J. L.; Geng, Y. H.; Yan, D. H. *Adv. Mater.* **2007**, *19*, 2168.
(11) Yang, J. L.; Wang, T.; Wang, H. B.; Zhu, F.; Li, G.; Yan, D. H. *J. Phys. Chem. B* **2008**, *112*, 3132.
(12) Wang, T.; Ebeling, D.; Yang, J. L.; Du, C. A.; Chi, L. F.; Fuchs, H.; Yan, D. H. *J. Phys. Chem. B* **2009**, *113*, 2333.
(13) Yang, J.; Yan, D. *Chem. Soc. Rev.* **2009**, *38*, 2634.

(14) Huang, L.; Zhu, F.; Liu, C.; Wang, H.; Geng, Y.; Yan, D. *Org. Electron.* **2010**, *11*, 195.

(15) Wang, H. B.; Song, D.; Yang, J. L.; Yu, B.; Geng, Y. H.; Yan, D. H. *Appl. Phys. Lett.* **2007**, *90*, 253510.

(16) Yu, B.; Huang, L.; Wang, H.; Yan, D. *Adv. Mater.* **2010**, *22*, 1017.

(17) Hotta, S.; Goto, M.; Azumi, R.; Inoue, M.; Ichikawa, M.; Taniguchi, Y. *Chem. Mater.* **2004**, *16*, 237.

(18) Ichikawa, M.; Yanagi, H.; Shimizu, Y.; Hotta, S.; Suganuma, N.; Koyama, T.; Taniguchi, Y. *Adv. Mater.* **2002**, *14*, 1272.

(19) Wang, H. B.; Wang, J.; Yan, X. J.; Shi, J. W.; Tian, H. K.; Geng, Y. H.; Yan, D. H. *Appl. Phys. Lett.* **2006**, *88*, 133508.

(20) Yang, J. L.; Wang, T.; Wang, H. B.; Zhu, F.; Li, G.; Yan, D. H. *J. Phys. Chem. B* **2008**, *112*, 7821.

(21) Kakudate, T.; Yoshimoto, N.; Saito, Y. *Appl. Phys. Lett.* **2007**, *90*, 081903.

(22) Zhang, X. N.; Barrena, E.; de Oteyza, D. G.; Dosch, H. *Surf. Sci.* **2007**, *601*, 2420.

(23) Hayakawa, R.; Zhang, X.; Dosch, H.; Hiroshiba, N.; Chikyow, T.; Wakayama, Y. *J. Phys. Chem. C* **2009**, *113*, 2197.

(24) Hotta, S.; Kimura, H.; Lee, S. A.; Tamaki, T. *J. Heterocycl. Chem.* **2000**, *37*, 281.

(25) Yang, J. L.; Wang, T.; Wang, H. B.; Zhu, F.; Li, G.; Yan, D. H. *J. Phys. Chem. B* **2008**, *112*, 7816.

(26) Jiang, Q.; Shi, H. X.; Zhao, M. *J. Chem. Phys.* **1999**, *111*, 2176.

(27) Ellison, C. J.; Torkelson, J. M. *Nat. Mater.* **2003**, *2*, 695.

(28) Lang, X. Y.; Zhang, G. H.; Lian, J. S.; Jiang, Q. *Thin Solid Films* **2006**, *497*, 333.

JP100095R